BBA - Biomembranes 1862 (2020) 183111

Contents lists available at ScienceDirect

BBA - Biomembranes

journal homepage: www.elsevier.com/locate/bbamem

Expression and detergent free purification and reconstitution of the plant plasma membrane Na^+/H^+ antiporter SOS1 overexpressed in *Pichia pastoris*☆

Debajyoti Dutta, Mansoore Esmaili, Michael Overduin, Larry Fliegel*

Department of Biochemistry, University of Alberta, Edmonton, Alberta T6G 2H7, Canada

ARTICLE INFO

Keywords:
Arabidopsis thaliana
Membrane protein
Na^+/H^+ antiporter
Protein purification
Liposome reconstitution
Pyranine
Salt tolerance
SOS1

ABSTRACT

The plant plasma membrane Na^+/H^+ antiporter SOS1 (Salt Overlay Sensitive 1) of *Arabidopsis thaliana* is the major transporter extruding Na^+ out of cells in exchange for an intracellular H^+. The sodium extrusion process maintains a low intracellular Na^+ concentration and thereby facilitates salt tolerance. *A. thaliana* SOS1 consists of 1146 amino acids, with the first 450 in a N-terminal membrane transport domain and the balance forming a cytosolic regulatory domain. For studies on characterization of the protein, two different constructs of SOS1 comprising of the residues 28 to 460 and 28 to 990 were cloned and overexpressed in methylotropic yeast strain of *Pichia pastoris* with a C-terminal histidine tag using the expression vector pPICZA. Styrene malic acid copolymers (SMA) were used as a cost-effective alternative to detergent for solubilization and isolation of this membrane protein. Immobilized Ni^{2+}-ion affinity chromatography was used to purify the expressed protein resulting in a yield of ~0.6–2 mg of SOS1 per liter of *Pichia pastoris* culture. The SMA purified protein containing amino acids 28 to 990 was directly reconstituted into liposomes for determination of Na^+ transport activity and was functionally active. However, similar reconstitution with amino acids 28–460 did not yield a functional protein. Other results have shown that the truncated SOS1 protein at amino acid 481 is active, which infers the presence of an element between residues 461–481 which is necessary for SOS1 activity. This region contains several conserved segments that may be important in SOS1 structure and function.

1. Introduction

Soil salinity is a major factor in reducing plant growth and productivity [1]. Most crop plants are highly sensitive to salt stress that causes a water deficit due to osmotic stress, and causes biochemical problems affecting plant growth rate, increase root to shoot ratio, and leaf damage [2–4]. Typically, plants maintain a relatively high intracellular K^+ (100–200 mM) and low Na^+ (1–10 mM). A key way that plants deal with Na^+ stress is to use the Salt Overlay Sensitive (SOS) signaling pathway that senses salt stress and takes preventive measures [5]. The major sodium transporting part of the SOS pathway is SOS1, that is a plasma membrane Na^+/H^+ antiporter that removes intracellular Na^+ in exchange for extracellular H^+. This secondary active transporter uses a proton gradient that is generated by the plasma membrane H^+-ATPase to remove intracellular sodium [6]. Plasma membrane SOS1 is predominantly expressed in the root and xylem to remove Na^+ out of the cell [6].

There are other types of cation/H^+ antiporters in plants including NHX8, intracellular Na^+/H^+ antiporters (NHXs) and CHXs. Intracellular Na^+/H^+ antiporters (NHXs) are expressed in intracellular organelles and are important in compartmentalization of salts, pH regulation, vesicle trafficking and [7]. $K^+(Na^+)/H^+$ antiporters (CHXs) are a large group of cation/H^+ antiporters some with obscure functions and some promoting membrane trafficking, endocytosis and growth and can also assist in dealing with salt stress [8]. While the functions of many plant cation/H^+ antiporters remain elusive, SOS1 deserves particular interest because it is well conserved and has a clear and simple role in enabling plant salt tolerance [4,9]. Overexpression of SOS1 has been shown to improve salt tolerance in plants [10] whereas conversely, inference with expression of SOS1 causes loss of halophytism [11]. The ability to confer salt tolerance by SOS1 even occurs across more distant species such as yeast. The salt-sensitive yeast *S. pombe* strain, that is deficient of endogenous plasma membrane Na^+/H^+ antiporter *Sp*NHE1, shows improved salt tolerance when *At*SOS1 is

☆ This article is part of a Special Issue entitled: Transporters in acidic organelles.

* Corresponding author at: Department of Biochemistry, 347 Medical Science Building, University of Alberta, Edmonton, Alberta T6G 2H7, Canada.
E-mail address: lfliegel@ualberta.ca (L. Fliegel).

https://doi.org/10.1016/j.bbamem.2019.183111
Received 12 July 2019; Received in revised form 22 October 2019; Accepted 24 October 2019
Available online 31 October 2019

expressed [12].

Membrane proteins are difficult to purify. They require solubilization from the membrane that is classically done with detergent. However, detergents and the process of solubilization have a number of disadvantages. The lipophilic character of membrane proteins means that when phospholipids are removed membrane proteins tend to aggregate and become inactive [13]. Detergents solubilize membrane protein but unlike phospholipids, they form micelles. Additionally, solubilization with a single detergent does not mimic phospholipid environmental complexity well and often, detergent solubilization fails to produce an active membrane protein [13]. Attempts to solubilize with detergent also suffer from an "open ended" protocol, in which many detergents must be tried repeatedly and with no defined working protocols [13,14]. Detergents often perturb interactions between proteins and subunits and their use can make it difficult to monitor proteins spectroscopically [13–16]. Finally, high detergent concentrations are needed throughout, making solubilization of large amounts of membrane protein costly.

New approaches are being developed allow proteins to be extracted with the surrounding lipid environment, with about 10–100 lipids in close contact. Several of these exist but require initial solubilization with detergent. Recently, an amphipathic polymer was developed to directly extract proteins from membranes. Styrene malic acid (SMA) copolymers with a statistical distribution of styrene and maleic acid monomers are a cost-effective alternative to detergents for membrane protein solubilization [17–19] but have not yet been shown to solubilize antiporters. By wrapping around a central disc of lipid bilayer, they provide structural organization and phase behavior to the section of membrane and are compatible with lipidic cubic phases for *in meso* crystallization [20–23] as well as cryo-electron microscopy studies of protein structures [24].

Here, we use an SMA that has a 2:1 ratio of styrene and maleic acid subunits to study the SOS1 protein. We overexpress and purify two different versions of plant plasma membrane Na^+/H^+ antiporter SOS1; one containing the predicted membrane transport domain with only10 amino acids from the C-terminal tail and the other containing the predicted membrane transport domain and 530 amino acids from the C-terminal cytoplasmic domain. The proteins are overexpressed in yeast *Pichia pastoris* and isolated and purified using SMA2000 polymer. The purified protein was successfully reconstituted into liposomes for determination of the metal/H^+ antiporter activity. The results represent the first report of SMA use for purification of this protein and for Na^+/H^+ exchangers in general and provide a rapid and inexpensive procedure for membrane protein production, purification and reconstitution.

2. Materials and methods

2.1. Sequence alignment and secondary structure prediction

Secondary structures and the disordered regions in the *At*SOS1 sequence were predicted using PSIPRED server [25,26]. Prediction of secondary structure was done using the GOR program [27].

2.2. Yeast expression system and vector for cloning

A modified pPICZA-eGFP vector was kindly provided by Dr. J. Lemieux (Dept. of Biochemistry, University of AB) [28]. In the modified vector, *Eco*RI and *Xho*I sites were replaced with *Pst*I and *Pvu*I respectively so that the final vector has *Pst*I and *Pvu*I sites between the alcohol oxidase promoter and the TEV coding sequence. Primers used for the modifications of the pPICZA-eGFP vector are summarized in Table 1.

2.3. Design of AtSOS1 constructs

Two different constructs of *At*SOS1 were made, one expressing amino acids 28–460 and another expressing amino acids 28–990 of *Arabidopsis thaliana* SOS1. Both were expressed with an added eGFP C-terminal tail separated by a TEV (Tobacco Etch Virus) cleavage site. For the $SOS1^{28–460}$ construct *At*SOS1 cDNA [12] was amplified using the primers SOSBPstIf and SOSBPvuIr (Table 1). For the $SOS1^{28–990}$ construct, *At*SOS1 cDNA was amplified using the primers SOSB*Pst*If and SOS990r. The amplified products and the vector were doubly digested with *Pst*I and *Pvu*I and inserts were ligated into the vector. Ligation products were amplified in *E. coli* strain DH5α. Final constructs were confirmed using DNA sequencing.

2.4. Yeast transformation and selection

Yeast transformation was done using an established protocol [29] with minor modifications. Briefly, pPICZA-SOS1-eGFP was linearized using the restriction enzyme *Pme*I. *Pichia pastoris* GS115 was grown in 100 ml YPD (1% Yeast extract, 2% Peptone, 2% Dextrose) to OD_{600} 1.0–1.5. Cells were harvested at 5000 rpm for 5 min. They were washed twice using ice-cold autoclaved distilled water and once with 1 M sterile sorbitol. Finally, cells were resuspended in 1 ml 1 M sorbitol and distributed into 80 µl aliquots in microfuge tubes. *Pme*I digested vector (10 µg; not exceeding 20 µ l in volume) was added to each aliquot and incubated for 5 min. The mixture was transferred to 0.2 cm gap size electroporation cuvettes and electroporation was with a Bio-Rad GenePulser with 2.1 kV, capacitance 25 µF, and resistance at 200 Ω. After electroporation 900 µl 1 M sorbitol was immediately added. The mixture was incubated for 1 h at 30 °C without shaking. Cells were then plated in YPDS (Yeast, Peptone, Dextrose, 1 M sorbitol) containing 200 µg ml^{-1}, 500 µg ml^{-1}, 1000 µg ml^{-1} or 2000 µg ml^{-1} zeocin. Selection plates were incubated for 4 days. Yeast colonies growing in the two highest concentrations of zeocin were grown BMMY (Buffered Methanol-complex Medium) agar plates for and examined for GFP fluorescence to identify high level expressing colonies [28].

2.5. Overexpression and purification of $SOS1^{28–460}$ and $SOS1^{28–990}$

High yielding *Pichia* clones were initially grown in 2 ml BMGY (Buffered Glycerol-complex Medium) overnight at 30 °C shaking. The following day the cells are inoculated to 50 ml BMGY media and grown to an OD_{600} of 6–7. Cells were harvested and washed with BMMY media once and inoculated into 4 L BMMY culture and grown for 3 days at 25 °C and agitated at 180 rpm. Methanol (0.5%) was added after 24 h. Antifoam 204 (Sigma A8311) 50 µl/500 ml culture was added [30]. Cells were then harvested and resuspended in 100 ml of buffer A (20 mM Tris pH 8.0, 200 mM NaCl, 5% glycerol), frozen quickly in liquid nitrogen and stored at −20 °C for no more then one week.

To lyse cells they were quickly thawed in warm water and subjected to three free-thaw cycles followed by addition of protease inhibitors (0.5 mM benzamidine, 100 µM leupeptin, 1 mM EDTA, 1.0 mM phenylmethanesulfonyl fluoride) and 1mM dithiothreitol. The following steps were performed on ice. The cell suspension was diluted to final 300 ml with buffer B (20 mM Tris pH 8.0, 200 mM NaCl, 10% glycerol) and sonication was performed using a probe sonnicator for 3 cycles with 2-s pulses and 5-s pauses (70% amplitude pulse). Unbroken cells were separated using 4000 × g for 10 min and supernatant was collected. The supernatant was subjected to centrifugation at 200,000 × *g* for 1 h to collect the membrane fraction and stored at −80 °C.

Eighty mg of membrane pellet was resuspended in buffer B and a stock solution of SMA2000 (Total Cray Valley) was added drop wise to a final concentration of 2.5% (w/v) where the final volume was 1 ml. The mixture was incubated at room temperature for 3 h with gentle agitation. The insoluble fraction was separated by centrifugation at 30,000 rpm for 30 min at 4 °C. The supernatant was filtered through a 400-micron syringe filter and incubated overnight with 10 ml of Ni-NTA resin (Qiagen), which was pre-equilibrated with buffer B. The next day, the flow through was collected and the column was washed with 3 × column volume of buffer B. Incubation was performed in presence

Table 1
Oligonucelotide primers used for cloning and mutagenesis. Bold indicates sequence varying from amplified template, italic lowercase indicates restriction enzyme site. Underlined indicates added initiator Met.

Primer	Sequence	Remark
ppicpspvF	**5′**-CTAATTATTCGAAACGA**G*ctgcag***ACGTGGCCCAGCC GGCCGTCTCGGATCGGTAC***cgatcg*** GAAAACCTGTACTTCC-**3′**	Forward primer, introduces *Pst*I and *Pvu*I sites before TEV-EGFP-8×-His in pPICZA vector
ppicpspvR	**5′**-GGAAGTACAGGTTTTC***cgatcg***GTACCGATCCGAGAC GGCCGGCTGGGCCACGT*ctgcag* CTCGTTTCGAATAATTAG-**3′**	Reverse primer, introduces *Pst*I and *Pvu*I sites before TEV-EGFP-8×-His in pPICZA vector
SosBPstIf	5′-CTTC***CtgcagAA*<u>ATG</u>**GCCAAACTAGAATCTAGCCCTG TCGACG-3′	Forward primer for SOS1^{28-} starts Lys^{28}; for cloning into modified pPICZA
SOSBPvuIr	5′-**GTTT*cgatcg***CTTGGGGGCTGGTAAAATATCCATGCG-3′	Reverse primer for amplification of SOS1 from Lys^{460}; for cloning into modified pPICZA
SOS990r	5′-***Ccgatcg***TGGTGTTAACGAAGATGGTCTTCGATGTAG-3′	Reverse primer for amplification of SOS1 from Pro^{990}; for cloning into modified pPICZA

of protease inhibitor cocktail [31], followed by 3× column volume of buffer C (20 mM Tris pH 8.0, 200 mM NaCl, 30 mM imidazole, 10% glycerol). Finally, the protein was eluted with buffer D (20 mM Tris pH 8.0, 200 mM NaCl, 300 mM imidazole, 10% glycerol). The eluted protein was concentrated using a Macrosep Advance Centrifugal Device with 30,000 molecular weight cut off (PALL Corporation) and dialyzed against buffer E (10 mM Bis-Tris Propane pH 7.5, 100 mM KCl, 10% glycerol) and flash frozen and stored at −80 °C. Finally, the protein concentration was measured with BioRad *DC*™ Protein assay kit against the dialysis buffer. In-gel GFP fluorescence images were taken using an ImageQuant LAS4000 equipped with blue light (GE Healthcare, USA). All exposures were taken at 1/2 of a second.

Mass spectrometry data was collected at the Alberta Proteomics and Mass Spectrometry Facility at the University of Alberta. In-gel trypsin digestion was performed on the samples. Briefly, excised gel bands were de-stained twice in 100 mM ammonium bicarbonate/acetonitrile (50:50), reduced (10 mM BME in 100 mM bicarbonate) and alkylated (55 mM iodoacetamide in 100 mM bicarbonate). After dehydration enough trypsin (6 ng/μl, Promega Sequencing grade) was added to just cover the gel pieces and the digestion was allowed to proceed overnight (~16 h) at room temperature. Tryptic peptides were initially extracted from the gel using 97% water:2% acetonitrile:1% formic acid followed by another extraction using 50% of the first extraction buffer and 50% acetonitrile.

Peptides were resolved and ionized by using nanoflow HPLC (Easy-nLC II, Thermo Scientific) with a PicoFrit fused silica capillary column (New Objective ProteoPepII, C18, 100 μm ID, 300 Å, 5 μm) coupled to an LTQ XL-Orbitrap hybrid mass spectrometer (Thermo Scientific). The samples were then injected onto the column at a flow rate of 3000 nl/min and resolved at 500 nl/min using a 60 min linear gradient from 0 to 35% v/v aqueous ACN in 0.2% v/v formic acid. The mass spectrometer was operated in data-dependent acquisition mode, recording high-accuracy and high-resolution survey Orbitrap spectra using external mass calibration, with a resolution of 30,000 and m/z range of 400–2000. The fourteen most intense multiply charged ions were sequentially fragmented by using collision induced dissociation, and spectra of their fragments were recorded in the linear ion trap; after two fragmentations all precursors selected for dissociation were dynamically excluded for 60 s. Data was processed using Proteome Discoverer 1.4 (Thermo Scientific) and databases were searched using SEQUEST (Thermo Scientific). Search parameters included a precursor mass tolerance of 10 ppm and a fragment mass tolerance of 0.8 Da. Peptides were searched with carbamidomethyl cysteine as a static modification and oxidized methionine, deamidated glutamine and asparagine as dynamic modifications.

2.6. Size exclusion chromatography

The protein was concentrated to more than 2 mg/ml and size fractionated on a Superdex 200 prep-grade matrix in a 16/70 column (GE Healthcare Biosciences) using a 0.7 ml/min flow rate in buffer B. For size exclusion chromatography the column was pre- equilibrated with buffer B and the processes were run in an AKTA Pure system with data collected with UNICORN 6.3 software (GE Healthcare Biosciences). The flow rate was maintained at 0.7 ml/min and 1 ml fractions were collected in a deep well block. All settings were kept constant throughout the experiment and calibration. The chromatogram was used to identify the protein containing fractions. Peak fractions were analyzed using SDS PAGE. For calibration of the column, Blue Dextran (2000 kDa), Thyroglobulin (669 kDa), Ferritin (440 kDa), Aldolase (158 kDa), BSA (66.5 kDa) were used. The calibration carve was plotted as retention volume (ml) vs. the log Mw.

2.7. Microscopy and GFP fluorescence

Confocal imaging of *P. pastoris* containing eGFP tagged *At*SOS1 constructs was performed in an Olympus IX81 microscope equipped with a spinning-disk optimized by Quorum Technologies (Guelph, ON, Canada). Images were obtained using Volocity software (Improvision Inc., Lexington, MA) with a 60× objective on a Hamamatsu EM-CCD camera (Hamamatsu, Japan). Yeast cells were either immobilized with 1% gelatin or used directly for live-cell imaging of the eGFP tag as described earlier [32].

2.8. Liposome preparation and protein reconstitution

Soy Asolectin (Sigma 11145) was washed twice with acetone and dissolved in chloroform. Chloroform dissolved lipid was dried in a glass tube under nitrogen flow to make a thin lipid film. The dried lipid was kept under vacuum overnight to remove residual chloroform. The next day, the lipid was dissolved in reconstitution buffer (10 mM Bis-Tris Propane pH 7.5, 25 mM NH_4Cl, 100 mM KCl, 10% glycerol) supplemented with pyranine (Sigma H1529) dye (2.5 mM) and then vortexed. The suspension was subjected to 5 freeze-thaw cycles. The lipid suspension was passed through a 400 μm track etched polycarbonate filter 19 times. The resulting suspension was incubated with freshly produced protein at a 100:1 lipid to protein ratio overnight. All long incubation steps were performed in an atmosphere of nitrogen (and reduced oxygen) to reduce lipid oxidation. The next day, $MgCl_2$ was added at a final concentration of 5 mM to precipitate the SMA [33] and after overnight incubation was centrifuged at 10000 ×g for 10 min to precipitate the unbound lipid and proteins. The supernatant was collected and dialyzed overnight against 500 X excess of the reconstitution buffer. Next day, the dialyzed suspension was collected and centrifuged at 265,000 ×g for 20 min to collect the liposomes. Liposomes were washed twice with reconstitution buffer and finally resuspended in 1 ml of reconstitution buffer and stored at 4 °C for not more then 5 days.

2.9. Cation transport assay

Na^+/H^+ exchanger activity was measured using a PTI Deltascan spectrofluorometer. Reconstituted or empty liposomes (prepared with

protein from yeast lysate with empty vector) were first examined to determine their excitation peak by scanning for emission with excitation at 463 nm. The peak pyranine emission was at 508 nm. Protein content in the proteoliposomes was quantified based on the SDS PAGE in-gel fluorescence. Pyranine was excited with the wavelength 463 nm and the emission was monitored at 508 nm. To assay Na^+/H^+ exchanger activity the proteoliposomes were diluted in ammonia free buffer containing 10 mM Bis-Tris Propane pH 7.5, 100 mM KCl, and 10% glycerol. They were incubated for 1.5 min until the system reaches equilibrium. A sodium gradient was added from outside and the changes in fluorescence were monitored for 5 min. Finally, the pH gradient was dissipated by the addition of NH_4Cl (25 mM). The data were plotted as Relative Fluorescence Vs. Time. Relative fluorescence is defined as $\frac{F - F_{min}}{F_{max} - F_{min}}$, where F = fluorescence, F_{min} = minimum fluorescence, F_{max} = maximum fluorescence. *Pichia pastoris* cells expressing an empty vector (pPICZa-TEV-eGFP) were used as control. Membranes were similarly purified from these cells and subjected to Ni-NTA chromatography purification to prepare the protein solution used as negative control of proteoliposomes (here referred to as empty vesicles).

3. Results

3.1. Design of SOS1 constructs spanning ordered regions

We examined the sequence of SOS1 using the server DISOPRED3 [26] to identify structured regions that are suitable for expression. The results (Fig. 1) showed that extreme N-terminus, an element following the last TM domain beginning at residue 460 and the C-terminal region beginning at amino acid 980 are likely to be highly disordered.

We constructed two *At*SOS1 constructs in a modified pPICZA vector under tight regulation of its methanol-induced promoter. Two constructs named SOS1460 and SOS1990 were designed that encode residues 28–460 and 28–990 of *At*SOS1, respectively. Both *At*SOS1 constructs include a C-terminal enhanced green fluorescent protein (eGFP) followed by a C-terminal His_8 tag to facilitate monitoring and purification of the expressed protein.

3.2. Overexpression and purification

We examined transformed yeast colonies for GFP fluorescence. Cloning of the plasmid vector into Pichia pastoris yielded with only a few colonies resistant to high Zeocin concentrations. GFP fluorescence could be detected within the cells and was apparently intracellular based on examination of GFP fluorescence and differential interference contrast microscopy images that compare the localization of expressed SOS1 proteins SOS460 and SOS990 to positive and negative controls that overexpress GFP alone or not GFP, respectively (Fig. 2).

Solubilization of the SOS1 proteins from Pichia membrane fractions was with SMA2000 (2.5% w/v). Solubilization was routinely performed at room temperature for 3 h that produced results equivalent to overnight incubation at 4 °C. Binding of the SMA solubilized SOS1-eGFP proteins to NTA-resins required overnight incubation. The complexes could only sustain washing concentrations of up to 30 mM imidazole. Washing the resin with higher imidazole concentrations led to leaching of the SOS1 proteins (data not shown). After washing the column with buffer B and with buffer B with 30 mM imidazole, SOS1 proteins were eluted with buffer B containing 300 mM imidazole yielding partial purification of SOS1 proteins (Fig. 3A, C). SOS1-eGFP proteins could be detected in SDS PAGE by in-gel fluorescence (Fig. 3B, D). The SOS460 and SOS990 proteins were found as bands at 55 and 125 kDa, respectively (Fig. 3A, C) and based on their calculated molecular weights of 76.6 and 136 kDa appear to be monomeric. Mass spectrometric analysis of other proteins present in the purified fractions identified two major contaminants. One protein of approximately 75 kDa in size is alcohol oxidase (Fig. 3A) and the other protein of approximately 130 kDa is the H^+-ATPase (Fig. 3C). The final yields of SOS460 and SOS990 were 2 and 0.6 mg of protein per liter of culture respectively. The differences can be attributed to degradation products that co-purified and contained eGFP as indicated by GFP fluorescence (Fig. 2B, D).

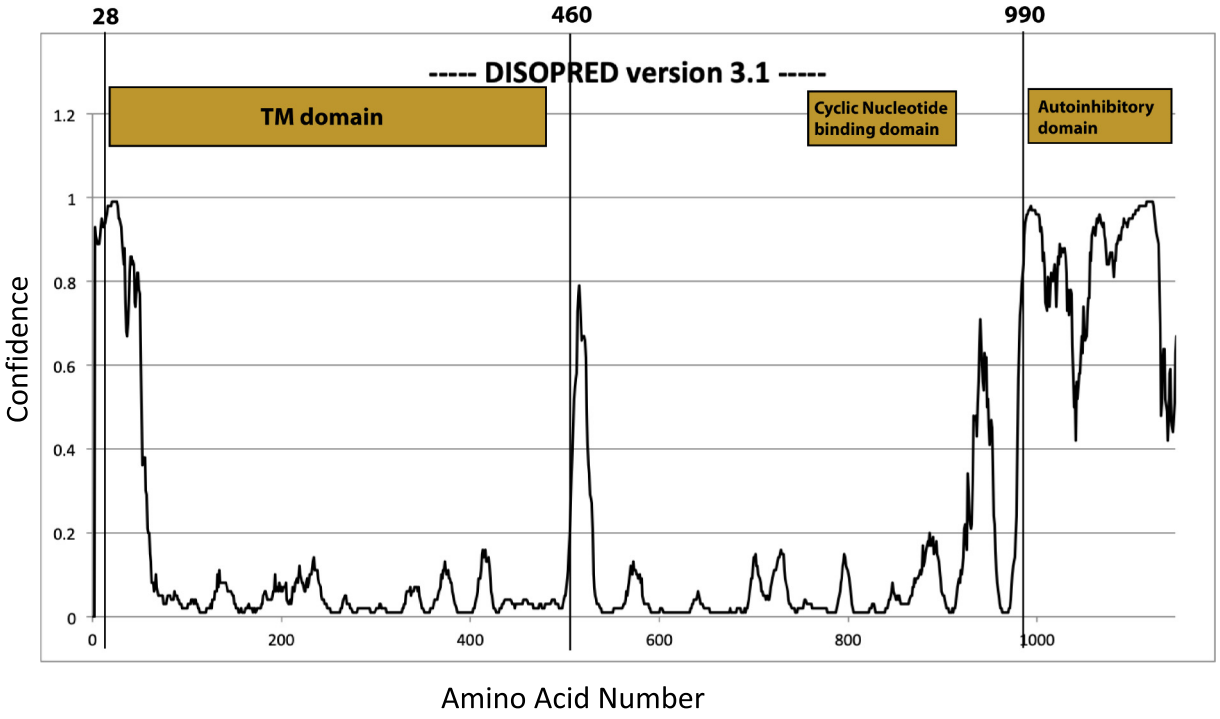

Fig. 1. Figure: Prediction of disordered regions of SOS1 using the server DISOPRED3 [26]. The X-axis shows the amino acid number and the Y-axis shows the confidence of disordered regions (highest = 1). Yellow boxes indicate the approximate amino acid spans of the transmembrane (TM) domain, cyclic nucleotide binding domain and the C-terminal autoinhibitory domain in the primary sequence. The start and end of the two constructs of SOS1 SOS460 and SOS990 (amino acids 28–460 and 28–990 respectively) used in this study are indicted.

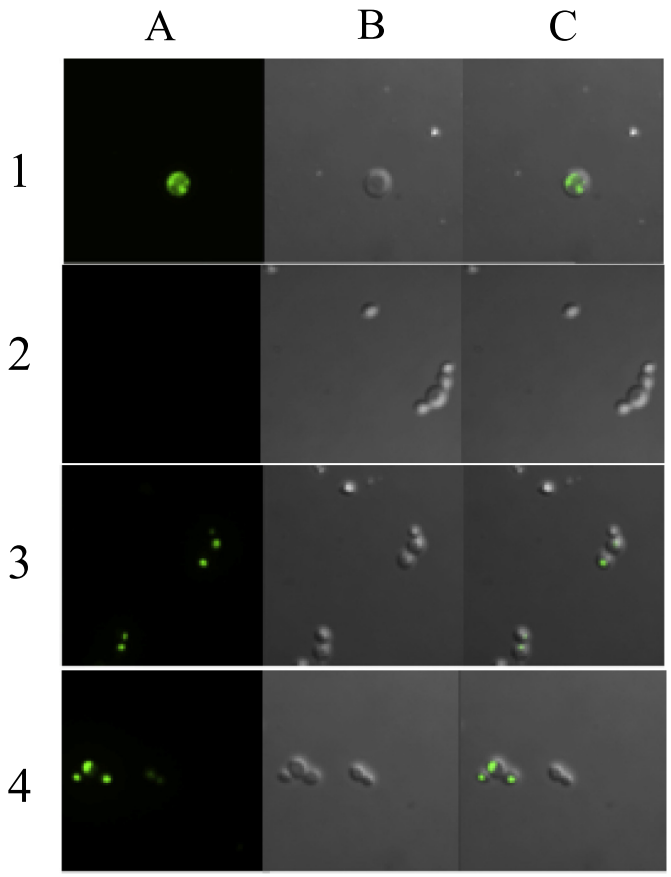

Fig. 2. Confocal images of *Pichia* expression constructs. A control and the SOS460 and SOS990 expression constructs were examined for GFP fluorescence to identify high level expressing colonies. Row 1–4: 1, Positive control; 2, Negative control; 3, SOS460; and 4, SOS990 expression in *Pichia*. Columns A–C: A, GFP fluorescence; B, Differential interference contrast microscopy; C, Merged A and B.

3.3. Gel exclusion chromatography

The *At*SOS1 proteins were further purified by gel exclusion chromatography (Fig. 4). Both SOS460 and SOS990 elution profiles show three major peaks: the first peaks elute at the void volume indicating an aggregation of the proteins. The peaks following correspond in size to the dimer or monomer fractions of SOS1. SDS-PAGE indicated that there was further enrichment of the SOS1 proteins. The SOS990 protein as well as alcohol oxidase were present in fractions 1–3 (Fig. 4C, D). Protein content of SOS460 increased in the third fraction compared to that of second fraction after size fractionation (Fig. 4C, D). It was the major band present in fractions 4–6, though alcohol oxidase was still present as a contaminant. When we re-loaded the middle peak of SOS990-eGFP, #2, onto the column again, and repeated size fractionation, again 3 peaks were found (not shown), suggesting that the peaks are in equilibrium with each other.

3.4. Reconstitution of SMALP-SOS into liposomes

To determine if the solubilized and partially purified SOS1 proteins were active, we reconstituted the proteins in soy asolectin (Fig. 5). Upon solubilization the majority of the SOS460 protein was released into the supernatant and was reconstituted into vesicles based on SDS-PAGE analysis (Fig. 5A, B). For the SOS460-SMALP, (Fig. 5A, B) solubilization of the protein resulted in the majority of the protein in the supernatant fraction. Reconstitution of the protein confirmed that it was present in the reconstituted vesicles. For the SOS990-SMALP we were also able to reconstitute the protein into vesicles though the amount of protein in the vesicles was less compared to SOS460. The Na^+/H^+ exchanger activity in the vesicle was triggered by addition of external NaCl and measured (Fig. 6) and demonstrates that the SOS990 protein was active. Addition of increasing amounts of NaCl initiated increasing amounts of Na^+/H^+ exchanger activity. Abolition of the pH gradient with NH_4Cl demonstrated that the system was functional and presented pH-dependent changes within the vesicle (Fig. 6A). Attempts to reconstitute functional SOS460 protein were unsuccessful (Fig. 6B), and demonstrated no significant activity over empty vesicles alone suggesting that elements outside its sequence are functionally critical.

3.5. Multiple sequence alignment of the SOS1 region 460–480

In order to identify potential conserved functional elements affecting protein activity in our study, the sequence of *At*SOS1 amino acids 429–481 was aligned with several plant SOS1 proteins and some yeast Na^+/H^+ antiporters that function in salt tolerance (Fig. 7). Comparison of the plant sequences reveals conserved elements including Leu-X-Tyr/Phe-Thr (where, X = Asp/Asn/Glu/Gln) and KYEMLNK sequences. These elements are found in the region between 460 and 480 which is missing in the SOS460 construct and which is predicted to be a helix using the GOR program [27]. The role of these regions is not known but could be structural or they may be involved in the transport process. Neither of these sequences is well conserved in the yeast antiporter sequences.

4. Discussion

4.1. Rationale approach to AtSOS1 expression

In this report we cloned, expressed and purified two different length clones of *At*SOS1. We chose amino acids 28–460 and 28–990 for expression for a number of reasons. Yeast plasma membrane Na^+/H^+ antiporters show significant homology with *At*SOS1 [34], and earlier studies have shown that yeast plasma membrane antiporters with C-terminal tails partially truncated, can still target properly to the plasma membrane and retain function [35,36]. Therefore, we reasoned that *At*SOS1 could also function with deletions in its large cytoplasmic tail. Specifically, for SOS460 this precise region was chosen for expression based on sequence alignment and secondary structure predictions that suggest that the putative transmembrane domain of AtSOS1 spans from the amino acid 34 to 448 [12]. Our analysis showed that the first 27 extracellular amino acids contain a low complexity serine-rich region (Fig. 1). Therefore, a short version of SOS1 was made by truncating the N-terminal residues 1 to 27 in conjugation with the truncation of the C-terminal residues from 461 to 1146. A short C-terminal segment 449–460 was retained to help ensure proper folding of the membrane domain, but this was terminated at amino acid 460 to avoid much of a disordered region of the C-terminal domain that immediately follows (Fig. 1).

A second construct SOS990 was designed to include both the membrane domain and much of the cytoplasmic domain. To decide how much of the large cytoplasmic domain to include, the secondary structure prediction and a computational prediction of the disordered regions of *At*SOS1 was examined. Our results (Fig. 1) suggested that residues 991 to 1146 possess a highly disordered region and possibly little rigid secondary structure. Hence, the larger version of *At*SOS1 was designed to end at amino acid 990 immediately prior to a large region of disordered protein. It is worth note that distal to amino acid 990 there is an autoinhibitory domain present and deletion of this domain can enhance SOS1 activity [37]. Therefore, this construct, while including a significant portion of the C-terminal, might have enhanced activity relative to the full-length protein.

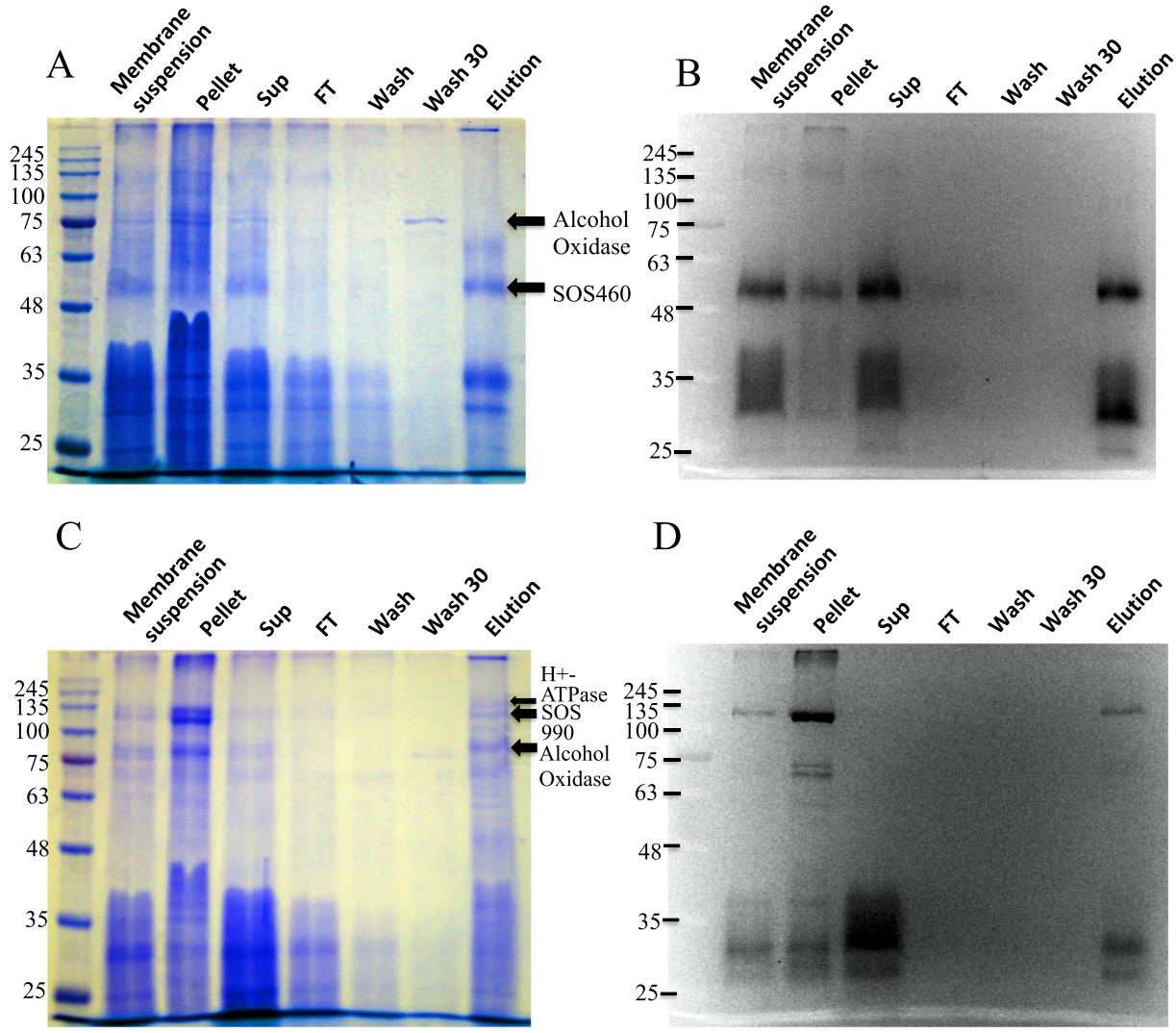

Fig. 3. SDS-PAGE (10%) analysis of SOS460 (A, B) and SOS990 (C, D). A, C, Coomassie Blue staining and B, D eGFP fluorescence. Arrows denote the position of SOS460 as well as, alcohol oxidase, and H^+-ATPase that were identified by mass spectroscopy. Pellet and supernatant (Sup) refer to the proteins after solubilization with SMA and centrifugation. FT, flow through that did not bind to the column after incubation. Wash refers to proteins obtained after washing columns with buffer B (20 mM Tris pH 8.0, 200 mM NaCl, 10% glycerol). Wash 30 was column wash with buffer B plus 30 mM imidazole. Elution was with buffer B plus 300 mM imidazole.

4.2. Expression and SMALP-based purification

We initially cloned the two forms of the *At*SOS1 protein SOS460 and SOS990 into a plasmid vector for expression in *Pichia pastoris*. *P. pastoris* has been reported to be a suitable host for high-level heterologous expression of plant proteins [38]. To express and purify *At*SOS1 we used the modified pPICZA vector that is under a tight regulation of a methanol-induced promoter. In the final plasmid constructs, *At*SOS1 coding sequences have a C-terminal eGFP (enhanced green fluorescent protein) that is followed by a C-terminal 8×-His tag. Protein expression was increased with antifoam usage and by growing the methanol induced cells at 26 °C. The plasmid was linearized and transformed into *Pichia* cells using electroporation. Initially, the transformants were selected using a high dose of antibiotic Zeocin and screened based on plating with methanol induction [28]. The GFP provides several advantages when studying membrane protein expression including enhancing folding of the protein and easier examination of expression and subcellular localization of the protein [39]. We obtained only a few colonies overall that were resistant to selection with Zeocin. Almost all the resistant colonies demonstrated high fluorescence, from the C-terminal GFP tag engineered onto the SOS1 proteins. Observation of the cells GFP fluorescence by confocal microscopy indicated that both SOS460 and SOS990 are expressed intracellularly and are localized in a granule like structure (Fig. 2). Such an expression pattern has also been seen for other recombinant expressed membrane proteins in *Pichia pastoris* [40,41]. It may be associated with GFP entering into growing peroxisomes during induction with methanol followed by insertion into densely packed layers of alcohol oxidase [40]. In fact, in our study we found that purified SOS1 proteins were associated with alcohol oxidase (Fig. 2) supporting this notion.

SMA2000 is an effective solubilizer of native membrane proteins bound to biological lipids [42]. SMA2000 at a concentration of 2.5% (w/v) was optimal in solubilization of the membrane proteins. However, SMA2000 was more effective in solubilizing SOS460 compared to SOS990 as most of the SOS990 protein remained in the pellet (Fig. 3C), whereas most of SOS460 was solubilized. Despite a variety of trials including increasing the concentration of SMA2000, the incubation time or the incubation temperature, none improved the SOS990 solubilization. SMA2000 is capable of solubilizing the 36 TM segments of AcrB [43,44]. In theory, SMA2000 should be able to solubilize the SOS1 membrane domain that is predicted to contain 13 transmembrane segments [12,45] and even as a dimer, should be accommodated within the ~10 nm diameters nanodiscs formed by SMA2000. This was, in fact, the case for SOS460. However, SOS990 solubilization was limited. The

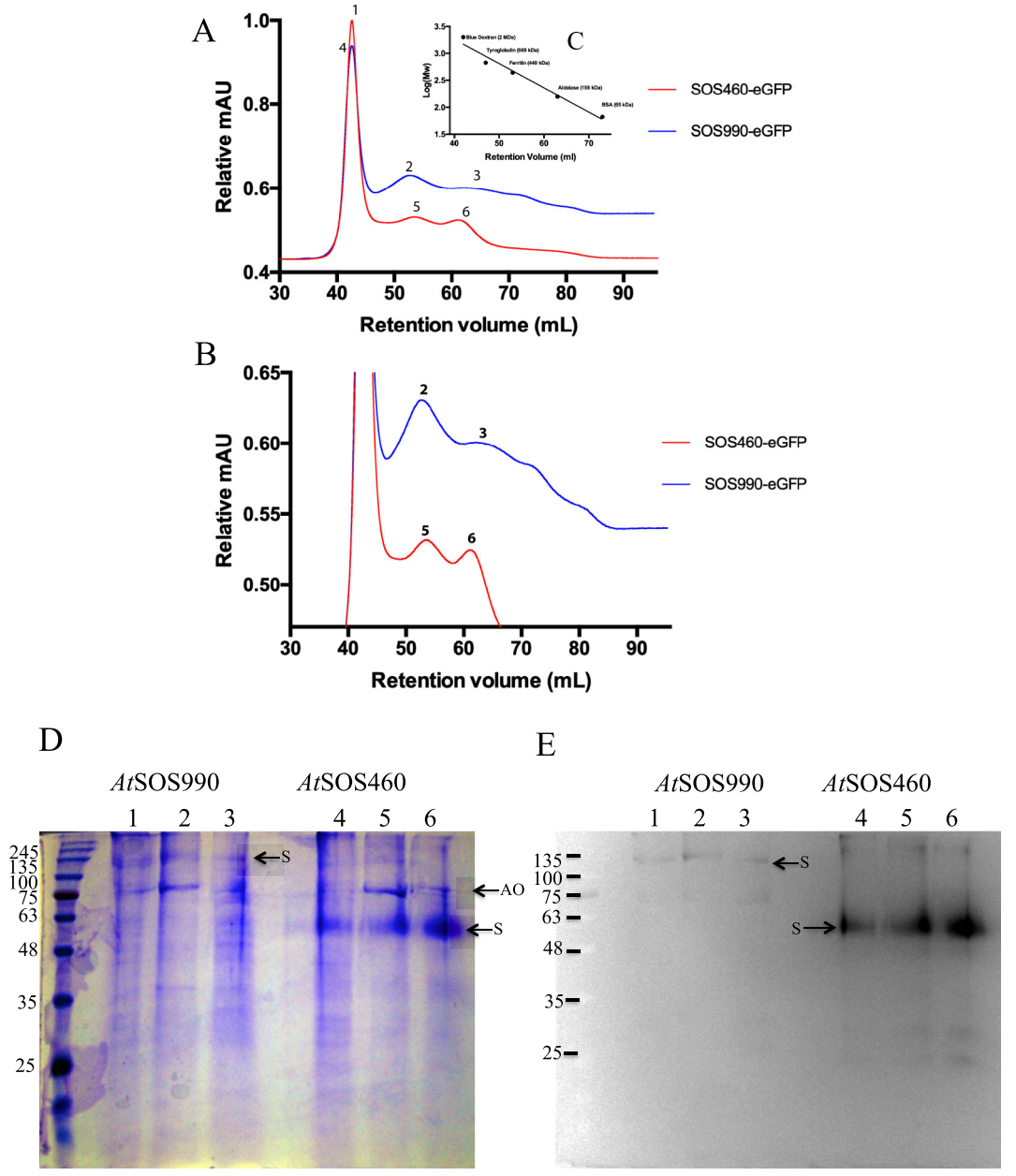

Fig. 4. Size exclusion chromatography profiles of partially purified SOS1 nanodiscs. Partially purified SOS460 and SOS990 proteins were fractionated on a Superdex 200 column as described in the "Materials and methods". A, fractionation of SOS1 proteins, SOS460 (red) and SOS990 (blue). X-axis marks the retention volumes and the Y-axis depicts the relative mAU. Aggregation peaks 1,4 are indicated. B, Closer view of peaks 2, 3, 5, and 6. C, Inset, calibration of the S200 column was shown. Molecular weight standards used were Blue Dextran (2000 kDa), Thyroglobulin (669 kDa), Ferritin (440 kDa), Aldolase (158 kDa) and Bovine Serum Albumin (65 kDa). D and E, SDS PAGE of peak fractions. Coomassie Blue staining (D) and in-gel fluorescence (E). Arrowheads denote alcohol oxidase (AO) and other arrowheads indicate the SOS1 proteins (S).

presence of the cytosolic domain may be responsible, as it may be tightly packed with the membrane domain [45], possibly increasing the volume of the membrane domain. Another reason could be an association of more lipids or contaminant proteins with SOS990 protein compared with SOS460.

Another difference between SMALP-SOS460 compared to SMALP-SOS990 was that with immobilized metal affinity chromatography, the SOS460 nanodiscs were purified to a higher degree than those of the SOS990 protein - though in neither case was the product completely purified with this one step procedure. For the SOS460 protein there were just three other major contaminating proteins, one of which was likely a fragment of SOS460 as it shows GFP fluorescence (Fig. 3).

Both SMALP solubilized SOS460 and SOS990 showed weak binding to the Ni-precast column. However, overnight incubation of the supernatant with the Ni-beads at 4 °C improved binding. We found 30 mM to be the maximum imidazole concentration in which the proteins remain bound to the column. Higher concentrations removed SOS460 and SOS990 from the column. Eluates of the protein contained contaminating alcohol oxidase. As noted above, this may be because the intracellular location of the SOS1 proteins residues where alcohol oxidase is found. Changing the metal used for affinity purification from Ni to Co did not improve protein purity, however prolonged washing (with resuspension buffer, 10 column volumes) in Ni-column following the 30 mM imidazole wash reduces the alcohol oxidase content in the eluted fraction (not shown). SDS-PAGE of the SOS-eGFP protein illustrated that the proteins run at a lower molecular weight than expected.

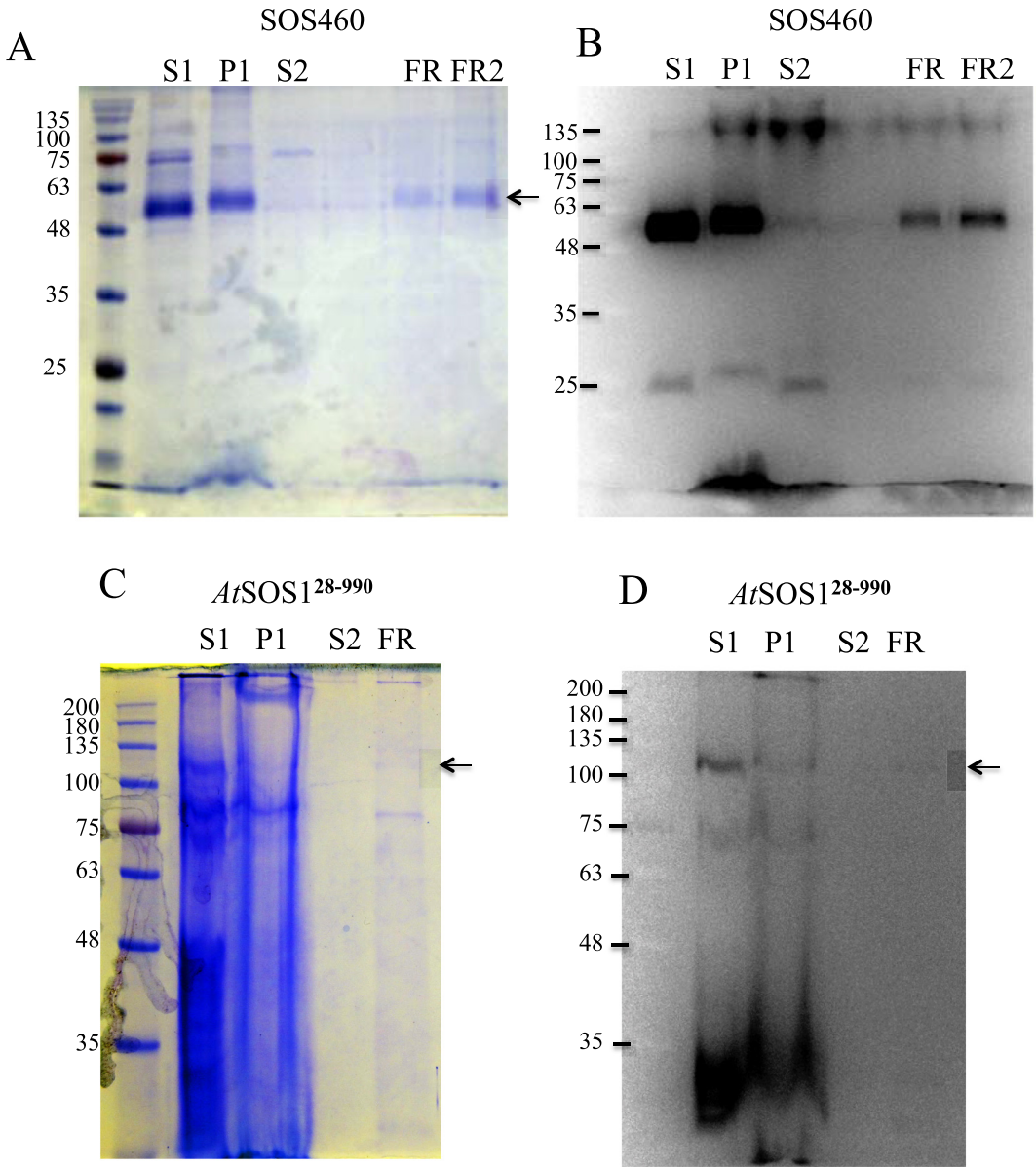

Fig. 5. Analysis of reconstituted SOS460 (A, B) and SOS990 (C, D) proteins by SDS-PAGE. Enriched SOS1 proteins were used after purification via immobilized metal affinity chromatography and size fractionation. Reconstitution into soy asolectin is shown, S1 = Starting protein solution, P1 = pellet from the first 10,000 ×*g* containing protein (in the presence of 5 mM $MgCl_2$) and lipid not solubilized and precipitated. S2, supernatant of 265,000 ×*g* spin. FR, final pellet after 265,000 ×*g* spin containing asolectin-protein vesicles. FR2, enriched fraction asolectin-protein vesicles.

This is typical of membrane proteins in SDS PAGE and in fact, we earlier found a similar migration pattern for SOS1-GFP constructs expressions in *S. pombe* [12].

Size fractionation of the SOS1 proteins led to further enrichment of the proteins, especially in the case of SOS460. In contrast, the SOS990 protein retained an association with several other proteins including several intermediate size or large molecular weight proteins (Fig. 4A–E). As with affinity chromatography, the yield and purity of the SOS460 was higher than that of the SOS990 protein. The protein content of the major elution peaks for SOS460 and SOS990 was examined by SDS-PAGE. Much of the SOS990 protein elutes in the void volume as putative aggregates, even though the calculated molecular weight is 136 kDa. The other two peaks at volume 52 ml (peak 2) and at 61 ml (peak 3) correspond to the molecular weights 525 kDa and 206 kDa respectively. Peaks 2 and 3 retained the contaminant alcohol oxidase (75 kDa). It has recently been shown that alcohol oxidase can form multiple stable oligomeric states [46]. We speculate that peak 2 may therefore contain a SOS990 dimer (270 kDa), which is contaminated with a tetramer of alcohol oxidase (300 kDa) whereas peak 3 may contain monomers of both the proteins. *At*SOS1 can also exist in monomeric form [45] so other combinations are possible. Minor variations in molecular weight could be due to lipid species associated with the proteins [47].

The protein SOS460 has a predicted molecular weight of 76.6 kDa. Its elution profile also revealed a major peak that is likely an aggregate of the protein (Fig. 4). There were also two other peaks at 53 ml (peak 5) and at 60 ml (peak 6) of approximate molecular weights of 473 kDa and 229 kDa. SDS PAGE confirms that alcohol oxidase also co-elutes with SOS460 in peak 5 and peak 6. In peak 5, SOS460 may elute as a dimer and possibly with an alcohol oxidase tetramer (300 kDa). In peak 6, SOS460 could be a dimer with an alcohol oxidase monomer.

The major difference between SOS990 and SOS460 is that in SMA2000 disc SOS990 exists in two populations, dimer and monomer whereas in SMA2000 disc SOS460 predominantly exists as a dimer. This

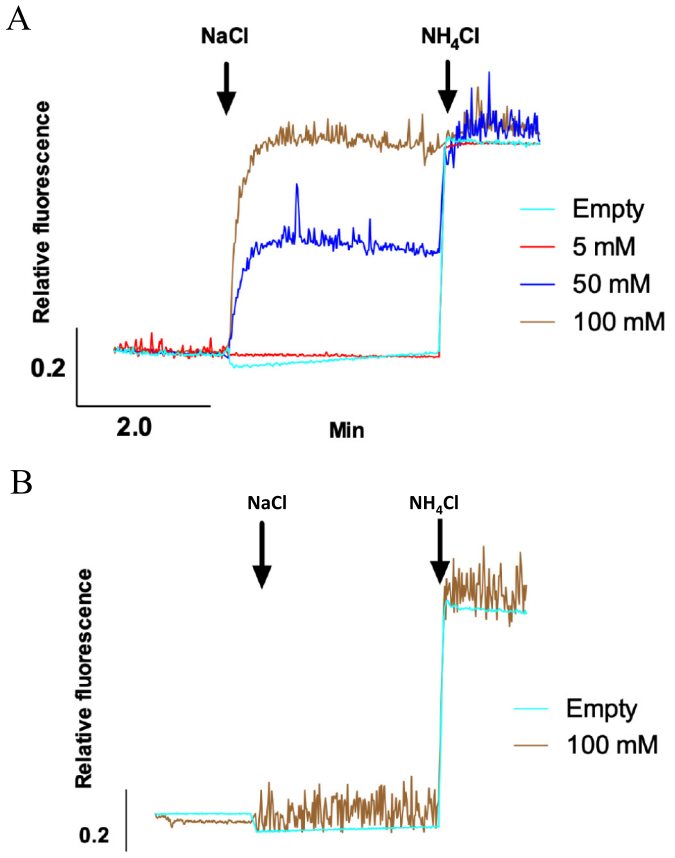

Fig. 6. Na^+/H^+ antiporter activity of liposome reconstituted SOS990 protein. A, The SOS990 protein was reconstituted as outlined in the "Materials and methods". NaCl was added to initiate activity in the indicated final concentrations. For empty vesicles 100 mM NaCl was added. (Empty vesicles were prepared from a cell lysate that did not have any protein expressed, with an empty expression vector.) NH_4Cl (25 mM) was added to dissipate the pH gradient after monitoring activity for 5 min. B, Similar analysis for SOS460 illustrating addition of 100 mM NaCl and empty vesicles (with 100 mM NaCl added).

supports the suggestion that the long C-terminus of SOS990 is possibly increasing the volume of the protein enough to bring it to the brink of the maximum SMA2000 disc size. On the other hand, the SOS460 dimer radius may fall more within the limit of SMA2000 disc size.

4.3. Reconstitution of SMALP-SOS1

Soy asolectin liposomes were prepared by freeze-thaw cycles followed by extrusion to obtain homogeneous distributions of the large unilameller vesicles with 400 nm diameters. This size of liposome was chosen to accommodate multiple copies of SOS1 into a single liposome thereby amplifying signal strength. Previous results have shown that proteins in SMA nanodiscs can be directly reconstituted into planar lipid bilayers yielding functional ion channels [48] and can be directly applied to obtain protein crystals from lipidic cubic phase crystallization trials [22]. A more recent report [49] demonstrated that it was possible to directly reconstitute SMA nanodiscs into liposomes without the use of detergent. SMA contamination has been reported to interfere with a protein's activity [49,50] so we were concerned that SMA contamination could interfere with proton transport activity of SOS1 in sealed vesicles. For this reason, our protocol was different from previously reported ones, and we incorporated a step with $MgCl_2$ incubation. The presence of $MgCl_2$ in concentrations over 4 mM results in SMA (and proteins) to precipitate out of solution liberating the nanodisc contents [33]. In our case, we found that approximately 90% of the *At*SOS1 proteins are precipitated after overnight incubation with 5 mM $MgCl_2$ (Fig. 5A, C, lane P1) and this step represented a major loss of protein. The supernatant of this step, the magnesium-containing supernatant, was dialyzed against magnesium free buffer. Dialysis served two purposes; it removes residual magnesium and generates sealed vesicles that were assayed for activity.

4.4. SOS1 activity in asolectin liposomes

We have previously demonstrated that *At*SOS1 with an eGFP tag is capable of conferring salt tolerance when expressed in a salt-sensitive mutant of *S. pombe*. This occurs even with a reduction in the size of the cytosolic tail [12]. In our present study, we therefore did not cleave GFP prior to its reconstitution into liposomes. The activity assay was performed by diluting ammonium chloride containing proteoliposomes, into ammonium chloride-free buffer. The release of free ammonia from within the proteoliposome generates an acidic internal pH. Empty liposomes were used as a control and were derived from incubating the liposomes with the protein purified from the empty vector expressing Pichia pastoris clone. These did not show any activity. SOS990-reconstituted proteoliposomes readily showed NaCl dependent Na^+/H^+ transport activity. Three different sodium concentrations (100 mM, 50 mM, and 5 mM) were tested to assay activity. The SOS990 protein showed a large rise of relative fluorescence at 100 mM and 50 mM while 5 mM Na did not initiate an increase in pyranine fluorescence compared to empty liposomes. The fluorescence changes reached maximum within about 1 min and thereafter a weak gradual decrease in relative fluorescence occurs (Fig. 6). The cause of the apparent reverse

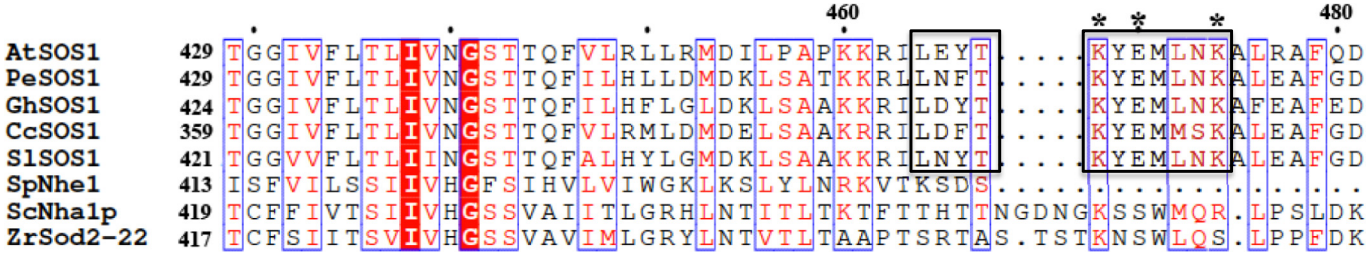

Fig. 7. Multiple sequence alignment of plasma membrane Na^+/H^+ antiporters aligned with proximal membrane *At*SOS1 region important in activity. *At*SOS1 (*Arabidopsis thaliana* SOS1; AAL32824), PeSOS1 (*Populus euphratica* SOS1; AQN76692.1), GhSOS1 (*Gossypium hirsutum* SOS1; AMY98958.1), CcSOS1 (*Chrysanthemum crassum* SOS1; BAR88076.1), SlSOS1 (*Solanum lycopersicum*; NP_001234698.2), SpNhe1 (*Schizosaccharomyces pombe* Nhe1; NP_592782.1), ScNha1p (*Saccharomyces cerevisiae*; XP_002497045.1), ZrSod2-22 (*Zygosaccharomyces rouxii* Sod2-22; XP_002497045.1). Red blocks are the conserved residues and the red coloured residues are amino acids of similar character. Conserved charged residues Lys468, Glu470, Lys474 are indicated by an asterisk. Boxes indicate conserved plant specific sequences in the 460–481 region including a Leu-X-Tyr/Phe-Thr sequence (where, X = Asp/Asn/Glu/Gln) and a LYEMLNK sequence that contains several charged residues.

transport is not known but could be due to some protein being reconstituted in the opposite orientation.

Despite the fact that we obtained a higher yield and purity of the SOS460 protein, and that it was clearly incorporated into the membrane vesicles, reconstituted SOS460 did not show any detectable Na^+/H^+ antiporter activity after addition of NaCl (Fig. 6B). We suggest the reason for the inactivity is the absence of C-terminal amino acids 461–480. Yeast plasma membrane Na^+/H^+ antiporters are the closest homologs of SOS1 in which structure-function correlations have been studied extensively [51–53]. The yeast alkali metal cation antiporter NHA1, is 985 amino acids and functions with most of its tail truncated and only 41 amino acids remaining after the last putative transmembrane domain [35]. Similar results were found for the *Saccharomyces cerevisiae* Na^+/H^+ exchanger Nha1p and *Candida tropicalis* Nha1p where deletion of most, but not all, of the large tail could be done before affecting the ability to confer salt tolerance [36,54]. In these cases, there appears to be a proximal region adjacent to the membrane domain that is essential for function, which may also be the case for *At*SOS1. Although SOS460 was inactive in our assays in another recent publication [12] another version of the SOS1 that terminated at amino acid 481, was found to be functional. It was able to confer salt tolerance when returned to a salt-sensitive strain of *S. pombe*. Together, the previous results and that of the present study, suggest that the residues 460–480 have a significant role in SOS1 activity. Fig. 7 shows that there are several sequences within this region that are conserved in plants, but not in yeast Na^+/H^+ antiporters. The role of these plant specific regions could be in interacting with the membrane and with the membrane domain itself to aid the ion transport. Future studies could examine this possibility.

Interestingly, recent results have shown a somewhat similar phenomenon occurs with the mammalian Na^+/H^+ exchanger NHE1 that is not highly homologous to SOS1. Human NHE1 is 815 amino acids in length with a 315 amino acid C-terminal tail and with amino acids 1–500 forming the membrane transport domain [55]. Truncation of the distal 80 amino acids of the tail of the protein leaves an active protein with only minor changes in regulation of activity. Further large reductions of the tail lead to defective cell surface targeting and increased protein degradation [56]. An NHE1 protein truncated at amino acid 543 was inactive [56] while ones truncated at amino acids 582 and 566 retained significant activity [57]. Thus it seems clear that, again, a proximal region near the membrane is necessary for activity. Future studies will examine this region in SOS1 in more detail.

Overall, our study has demonstrated that the SOS1 protein can be expressed in *Pichia pastoris* in functional form, when the cytosolic tail is included. Reduction of the tail of the protein to amino acid 460, made the resultant protein inactive. In this study, we were able to use a detergent-free procedure that differs from a previous study [45]. The advantages of the detergent free protocols are many. Firstly, there is a greatly reduced cost. Attempts to solubilize and purify proteins with detergents can lead to many expensive trials [13,14]. Additionally, interactions between detergents and regulatory proteins are often perturbed by detergents [13,15,16]. Detergents are also more denaturing than styrene-maleic acid co-polymers and will remove associated lipids that can remain bound in nanodiscs that SMA's form [48]. Our work leads to future studies will attempt further purification and structural determination of SOS1 and may examine associated proteins and lipids.

Acknowledgements

LF and DD were supported for this work by a grant from NSERC #RGPIN-2014-06564. MO and ME were supported for this work by the Campus Alberta Innovation Program (RCP-12-002C), Alberta Prion Research Institute/Alberta Innovates Bio Solutions (201600018), NSERC RGPIN-2018-04994 and TMIC The Metabolomics Innovation Centre grants.

References

[1] W. Wang, B. Vinocur, A. Altman, Plant responses to drought, salinity and extreme temperatures: towards genetic engineering for stress tolerance, Planta 218 (2003) 1–14.
[2] W.B. Frommer, U. Ludewig, D. Rentsch, Taking transgenic plants with a pinch of salt, Science 285 (1999) 1222–1223.
[3] M.P. Apse, E. Blumwald, Engineering salt tolerance in plants, Curr. Opin. Biotechnol. 13 (2002) 146–150.
[4] U. Deinlein, A.B. Stephan, T. Horie, W. Luo, G. Xu, J.I. Schroeder, Plant salt-tolerance mechanisms, Trends Plant Sci. 19 (2014) 371–379.
[5] H. Ji, J.M. Pardo, G. Batelli, M.J. Van Oosten, R.A. Bressan, X. Li, The Salt Overly Sensitive (SOS) pathway: established and emerging roles, Mol. Plant 6 (2013) 275–286.
[6] H. Shi, F.J. Quintero, J.M. Pardo, J.K. Zhu, The putative plasma membrane Na(+)/H(+) antiporter SOS1 controls long- distance Na(+) transport in plants, Plant Cell 14 (2002) 465–477.
[7] M.P. Rodriguez-Rosales, F.J. Galvez, R. Huertas, M.N. Aranda, M. Baghour, O. Cagnac, K. Venema, Plant NHX cation/proton antiporters, Plant Signal. Behav. 4 (2009) 265–276.
[8] H. Sze, S. Chanroj, Plant endomembrane dynamics: studies of K(+)/H(+) antiporters provide insights on the effects of pH and ion homeostasis, Plant Physiol. 177 (2018) 875–895.
[9] M. Hanin, C. Ebel, M. Ngom, L. Laplaze, K. Masmoudi, New insights on plant salt tolerance mechanisms and their potential use for breeding, Front. Plant Sci. 7 (2016) 1787.
[10] H. Shi, B.H. Lee, S.J. Wu, J.K. Zhu, Overexpression of a plasma membrane Na+/H+ antiporter gene improves salt tolerance in Arabidopsis thaliana, Nat. Biotechnol. 21 (2003) 81–85.
[11] D.H. Oh, E. Leidi, Q. Zhang, S.M. Hwang, Y. Li, F.J. Quintero, X. Jiang, M.P. D'Urzo, S.Y. Lee, Y. Zhao, J.D. Bahk, R.A. Bressan, D.J. Yun, J.M. Pardo, H.J. Bohnert, Loss of halophytism by interference with SOS1 expression, Plant Physiol. 151 (2009) 210–222.
[12] A. Ullah, D. Dutta, L. Fliegel, Expression and characterization of the SOS1 Arabidopsis salt tolerance protein, Mol. Cell. Biochem. 415 (2016) 133–143.
[13] S.C. Lee, T.J. Knowles, V.L. Postis, M. Jamshad, R.A. Parslow, Y.P. Lin, A. Goldman, P. Sridhar, M. Overduin, S.P. Muench, T.R. Dafforn, A method for detergent-free isolation of membrane proteins in their local lipid environment, Nat. Protoc. 11 (2016) 1149–1162.
[14] J. Kellosalo, T. Kajander, R. Honkanen, A. Goldman, Crystallization and preliminary X-ray analysis of membrane-bound pyrophosphatases, Mol. Membr. Biol. 30 (2013) 64–74.
[15] C. Breyton, C. Tribet, J. Olive, J.P. Dubacq, J.L. Popot, Dimer to monomer conversion of the cytochrome b6 f complex. Causes and consequences, J. Biol. Chem. 272 (1997) 21892–21900.
[16] M. Esmann, Solubilized (Na+ + K+)-ATPase from shark rectal gland and ox kidney—an inactivation study, Biochim. Biophys. Acta 857 (1986) 38–47.
[17] T.J. Knowles, R. Finka, C. Smith, Y.P. Lin, T. Dafforn, M. Overduin, Membrane proteins solubilized intact in lipid containing nanoparticles bounded by styrene maleic acid copolymer, J. Am. Chem. Soc. 131 (2009) 7484–7485.
[18] M. Jamshad, J. Charlton, Y.P. Lin, S.J. Routledge, Z. Bawa, T.J. Knowles, M. Overduin, N. Dekker, T.R. Dafforn, R.M. Bill, D.R. Poyner, M. Wheatley, G-protein coupled receptor solubilization and purification for biophysical analysis and functional studies, in the total absence of detergent, Biosci. Rep. 35 (2015).
[19] N.L. Pollock, S.C. Lee, J.H. Patel, A.A. Gulamhussein, A.J. Rothnie, Structure and function of membrane proteins encapsulated in a polymer-bound lipid bilayer, Biochim. Biophys. Acta Biomembr. 1860 (2018) 809–817.
[20] M. Jamshad, V. Grimard, I. Idini, T.J. Knowles, M.R. Dowle, N. Schofield, P. Sridhar, Y. Lin, R. Finka, M. Wheatley, O.R.T. Thomas, R.E. Palmer, M. Overduin, C. Govaerts, J.-M. Ruysschaert, K.J. Edler, T.R. Dafforn, Structural analysis of a nanoparticle containing a lipid bilayer used for detergent-free extraction of membrane proteins, Nano Res. 8 (2015) 774–789.
[21] S. Scheidelaar, M.C. Koorengevel, J.D. Pardo, J.D. Meeldijk, E. Breukink, J.A. Killian, Molecular model for the solubilization of membranes into nanodisks by styrene maleic acid copolymers, Biophys. J. 108 (2015) 279–290.
[22] J. Broecker, B.T. Eger, O.P. Ernst, Crystallogenesis of membrane proteins mediated by polymer-bounded lipid nanodiscs, Structure 25 (2017) 384–392.
[23] J.M. Dorr, M.H. van Coevorden-Hameete, C.C. Hoogenraad, J.A. Killian, Solubilization of human cells by the styrene-maleic acid copolymer: insights from fluorescence microscopy, Biochim. Biophys. Acta Biomembr. 1859 (2017) 2155–2160.
[24] C. Sun, S. Benlekbir, P. Venkatakrishnan, Y. Wang, S. Hong, J. Hosler, E. Tajkhorshid, J.L. Rubinstein, R.B. Gennis, Structure of the alternative complex III in a supercomplex with cytochrome oxidase, Nature 557 (2018) 123–126.
[25] D.W. Buchan, F. Minneci, T.C. Nugent, K. Bryson, D.T. Jones, Scalable web services for the PSIPRED protein analysis workbench, Nucleic Acids Res. 41 (2013) W349–W357.
[26] D.T. Jones, D. Cozzetto, DISOPRED3: precise disordered region predictions with annotated protein-binding activity, Bioinformatics 31 (2015) 857–863.
[27] C. Combet, C. Blanchet, C. Geourjon, G. Deleage, NPS@: network protein sequence analysis, Trends Biochem. Sci. 25 (2000) 147–150.
[28] C.L. Brooks, M. Morrison, M.J. Lemieux, Rapid expression screening of eukaryotic membrane proteins in Pichia pastoris, Protein Sci. 22 (2013) 425–433.
[29] M. Weidner, M. Taupp, S.J. Hallam, Expression of recombinant proteins in the methylotrophic yeast Pichia pastoris, J. Vis. Exp. (2010) e1862, , https://doi.org/

10.3791/1862.
[30] Y. Zhong, L. Yang, Y. Guo, F. Fang, D. Wang, R. Li, M. Jiang, W. Kang, J. Ma, J. Sun, W. Xiao, High-temperature cultivation of recombinant Pichia pastoris increases endoplasmic reticulum stress and decreases production of human interleukin-10, Microb. Cell Factories 13 (2014) 163.
[31] N.L. Silva, H. Wang, C.V. Harris, D. Singh, L. Fliegel, Characterization of the Na^+/H^+ exchanger in human choriocarcinoma (BeWo) cells, Pflugers Archiv Eur. J. Physiol. 433 (1997) 792–802.
[32] L. Fliegel, C. Wiebe, G. Chua, P.G. Young, Functional expression and cellular localization of the Na+/H+ exchanger Sod2 of the fission yeast Schizosaccharomyces pombe, Can. J. Physiol. Pharmacol. 83 (2005) 565–572.
[33] K.A. Morrison, A. Akram, A. Mathews, Z.A. Khan, J.H. Patel, C. Zhou, D.J. Hardy, C. Moore-Kelly, R. Patel, V. Odiba, T.J. Knowles, M.U. Javed, N.P. Chmel, T.R. Dafforn, A.J. Rothnie, Membrane protein extraction and purification using styrene-maleic acid (SMA) copolymer: effect of variations in polymer structure, Biochem. J. 473 (2016) 4349–4360.
[34] D. Dutta, L. Fliegel, Structure and function of yeast and fungal Na(+)/H(+) antiporters, IUBMB Life 70 (2018) 23–31.
[35] O. Kinclova, J. Ramos, S. Potier, H. Sychrova, Functional study of the Saccharomyces cerevisiae Nha1p C-terminus, Mol. Microbiol. 40 (2001) 656–668.
[36] K. Mitsui, S. Kamauchi, N. Nakamura, H. Inoue, H. Kanazawa, A conserved domain in the tail region of the Saccharomyces cerevisiae Na+/H+ antiporter (Nha1p) plays important roles in localization and salinity-resistant cell-growth, J. Biochem. 135 (2004) 139–148.
[37] F.J. Quintero, J. Martinez-Atienza, I. Villalta, X. Jiang, W.Y. Kim, Z. Ali, H. Fujii, I. Mendoza, D.J. Yun, J.K. Zhu, J.M. Pardo, Activation of the plasma membrane Na/H antiporter Salt-Overly-Sensitive 1 (SOS1) by phosphorylation of an auto-inhibitory C-terminal domain, Proc. Natl. Acad. Sci. U. S. A. 108 (2011) 2611–2616.
[38] F. Yesilirmak, Z. Sayers, Heterelogous expression of plant genes, Int. J. Plant Genomics 296482 (2009).
[39] E.R. Geertsma, M. Groeneveld, D.J. Slotboom, B. Poolman, Quality control of overexpressed membrane proteins, Proc. Natl. Acad. Sci. U. S. A. 105 (2008) 5722–5727.
[40] A.L. Zupan, S. Trobec, V. GabercPorekar, High expression of green fluorescent protein in Pichia pastoris leads to formation of fluorescent particles, J. Biotechnol. 109 (2004) 115–122.
[41] T. Vogl, G.G. Thallinger, G. Zellnig, D. Drew, J.M. Cregg, A. Glieder, M. Freigassner, Towards improved membrane protein production in Pichia pastoris: general and specific transcriptional response to membrane protein overexpression, New Biotechnol. 31 (2014) 538–552.
[42] S. Paulin, M. Jamshad, T.R. Dafforn, J. Garcia-Lara, S.J. Foster, N.F. Galley, D.I. Roper, H. Rosado, P.W. Taylor, Surfactant-free purification of membrane protein complexes from bacteria: application to the staphylococcal penicillin-binding protein complex PBP2/PBP2a, Nanotechnology 25 (2014) 285101.
[43] W. Qiu, Z. Fu, G.G. Xu, R.A. Grassucci, Y. Zhang, J. Frank, W.A. Hendrickson, Y. Guo, Structure and activity of lipid bilayer within a membrane-protein transporter, Proc. Natl. Acad. Sci. U. S. A. 115 (2018) 12985–12990.
[44] V. Postis, S. Rawson, J.K. Mitchell, S.C. Lee, R.A. Parslow, T.R. Dafforn, S.A. Baldwin, S.P. Muench, The use of SMALPs as a novel membrane protein scaffold for structure study by negative stain electron microscopy, Biochim. Biophys. Acta 1848 (2015) 496–501.
[45] R. Nunez-Ramirez, M.J. Sanchez-Barrena, I. Villalta, J.F. Vega, J.M. Pardo, F.J. Quintero, J. Martinez-Salazar, A. Albert, Structural insights on the plant salt-overly-sensitive 1 (SOS1) Na(+)/H(+) antiporter, J. Mol. Biol. 424 (2012) 283–294.
[46] J. Vonck, D.N. Parcej, D.J. Mills, Structure of alcohol oxidase from Pichia pastoris by cryo-electron microscopy, PLoS One 11 (2016) e0159476.
[47] E. Folta-Stogniew, Oligomeric states of proteins determined by size-exclusion chromatography coupled with light scattering, absorbance, and refractive index detectors, Methods Mol. Biol. 328 (2006) 97–112.
[48] J.M. Dorr, M.C. Koorengevel, M. Schafer, A.V. Prokofyev, S. Scheidelaar, E.A. van der Cruijsen, T.R. Dafforn, M. Baldus, J.A. Killian, Detergent-free isolation, characterization, and functional reconstitution of a tetrameric K+ channel: the power of native nanodiscs, Proc. Natl. Acad. Sci. U. S. A. 111 (2014) 18607–18612.
[49] I.A. Smirnova, P. Adelroth, P. Brzezinski, Extraction and liposome reconstitution of membrane proteins with their native lipids without the use of detergents, Sci. Rep. 8 (2018) 14950.
[50] Y. Liu, E. Moura, J.M. Dorr, S. Scheidelaar, M. Heger, M.R. Egmond, J.A. Killian, T. Mohammadi, E. Breukink, Bacillus subtilis MraY in detergent-free system of nanodiscs wrapped by styrene-maleic acid copolymers, PLoS One 13 (2018) e0206692.
[51] A. Ullah, G. Kemp, B. Lee, C. Alves, H. Young, B.D. Sykes, L. Fliegel, Structural and functional analysis of transmembrane segment IV of the salt tolerance protein Sod2, J. Biol. Chem. 288 (2013) 24609–24624.
[52] O. Kinclova-Zimmermannova, P. Falson, D. Cmunt, H. Sychrova, A hydrophobic filter confers the cation selectivity of Zygosaccharomyces rouxii plasma-membrane Na+/H+ antiporter, J. Mol. Biol. 427 (2015) 1681–1694.
[53] D. Dutta, K. Shin, J.K. Rainey, L. Fliegel, Transmembrane segment XI of the Na(+)/H(+) antiporter of S. pombe is a critical part of the ion translocation pore, Sci. Rep. 7 (2017) 12793.
[54] S. Kamauchi, K. Mitsui, S. Ujike, M. Haga, N. Nakamura, H. Inoue, S. Sakajo, M. Ueda, A. Tanaka, H. Kanazawa, Structurally and functionally conserved domains in the diverse hydrophilic carboxy-terminal halves of various yeast and fungal Na/H antiporters (Nha1p), J. Biochem. (Tokyo) 131 (2002) 821–831.
[55] D. Dutta, L. Fliegel, Molecular modeling and inhibitor docking analysis of the Na+/H+ exchanger isoform one, Biochem. Cell Biol. 97 (2018) 333–343.
[56] X. Li, A. Augustine, S. Chen, L. Fliegel, Stop codon polymorphisms in the human SLC9A1 gene disrupt or compromise Na+/H+ exchanger function, PLoS One 11 (2016) e0162902.
[57] L. Bianchini, A. Kapus, G. Lukacs, S. Wasan, S. Wakabayashi, J. Pouyssegur, F.H. Yu, J. Orlowski, S. Grinstein, Responsiveness of mutants of NHE1 isoform of Na^+/H^+ antiport to osmotic stress, Am. J. Phys. 269 (1995) C998–C1007.